University Library

MINERVA ACCESS

A gateway to Melbourne's research publications

Minerva Access is the Institutional Repository of The University of Melbourne

Author/s:
Wurdack, M;Yun, T;Estrecho, E;Syed, N;Bhattacharyya, S;Pieczarka, M;Zavabeti, A;Chen, SY;Haas, B;Müller, J;Lockrey, MN;Bao, Q;Schneider, C;Lu, Y;Fuhrer, MS;Truscott, AG;Daeneke, T;Ostrovskaya, EA

Title:
Ultrathin Ga2O3 Glass: A Large-Scale Passivation and Protection Material for Monolayer WS2

Date:
2021-01-01

Citation:
Wurdack, M., Yun, T., Estrecho, E., Syed, N., Bhattacharyya, S., Pieczarka, M., Zavabeti, A., Chen, S. Y., Haas, B., Müller, J., Lockrey, M. N., Bao, Q., Schneider, C., Lu, Y., Fuhrer, M. S., Truscott, A. G., Daeneke, T. & Ostrovskaya, E. A. (2021). Ultrathin Ga2O3 Glass: A Large-Scale Passivation and Protection Material for Monolayer WS2. Advanced Materials, 33 (3), https://doi.org/10.1002/adma.202005732.

Persistent Link:
https://hdl.handle.net/11343/276700

Ultrathin Ga_2O_3 glass: A large scale passivation and protection material for monolayer WS_2

Matthias Wurdack, Tinghe Yun, Eliezer Estrecho, Nitu Syed, Semonti Bhattacharyya, Maciej Pieczarka, Ali Zavabeti, Shao-Yu Chen, Benedikt Haas, Johannes Müller, Mark N. Lockrey, Qiaoliang Bao, Christian Schneider, Yuerui Lu, Michael S. Fuhrer, Andrew G. Truscott, Torben Daeneke*, Elena A. Ostrovskaya**

M. Wurdack, T. Yun, Dr. E. Estrecho, Dr. S. Bhattacharyya, Dr. M. Pieczarka, Dr. S.-Y. Chen, A/Prof. Y. Lu, Prof. M. S. Fuhrer, Dr. T. Daeneke, Prof. E. A. Ostrovskaya
ARC Centre of Excellence in Future Low-Energy Electronics Technologies
E-mail: matthias.wurdack@anu.edu.au, torben.daeneke@rmit.edu.au, elena.ostrovskaya@anu.edu.au

M. Wurdack, Dr. E. Estrecho, Dr. M. Pieczarka, Prof. E. A. Ostrovskaya
Nonlinear Physics Centre, Research School of Physics, The Australian National University, Canberra, ACT 2601, Australia

T. Yun, A/Prof. Q. Bao
Department of Materials Science and Engineering, Monash University, Clayton, Australia

Dr. N. Syed, Dr. A. Zavabeti, Dr. T. Daeneke
Department of Chemical and Environmental Engineering, RMIT, Melbourne, Australia

Dr. S. Bhattacharyya, Dr. S.-Y. Chen, Prof. M. S. Fuhrer
School of Physics and Astronomy, Monash University, Clayton, Australia

Dr. A. Zavabeti
Department of Chemical Engineering, The University of Melbourne, Parkville, VIC, 3010, Australia

Dr. B. Haas, J. Müller
Institut fur Physik & IRIS Adlershof, Humboldt-Universität zu Berlin, D-10099 Berlin, Germany

Dr. M. N. Lockrey
School of Mathematical and Physical Sciences, University of Technology Sydney, Ultimo, NSW 2007 Australia

Prof. C. Schneider
Institut of Physics, Carl von Ossietzky University of Oldenburg, Ammerländer Heerstrasse 114-118, 26126 Oldenburg, Germany

A/Prof. Y. Lu
Research School of Electrical, Energy and Materials Engineering, College of Engineering and Computer Science, The Australian National University, Canberra, ACT 2601, Australia

Prof. A. G. Truscott
Laser Physics Centre, Research School of Physics, The Australian National University,Canberra, ACT 2601,

Keywords: *Two-dimensional materials, atomically-thin semiconductors, transition metal dichalcogenides, exciton enhancement, passivation, device integration*

Atomically thin transition metal dichalcogenide crystals (TMDCs) have extraordinary optical properties that make them attractive for future optoelectronic applications. Integration of TMDCs into practical all-dielectric heterostructures hinges on the ability to passivate and protect them against necessary fabrication steps on large scales. Despite its limited scalability, encapsulation of TMDCs in hexagonal boron nitride (hBN) currently has no viable alternative for achieving high performance of the final device. Here, we show that the novel, ultrathin Ga_2O_3 glass is an ideal centimeter-scale coating material that enhances optical performance of the monolayers and protects them against further material deposition. In particular, Ga_2O_3 capping of monolayer WS_2 outperforms commercial grade hBN in both scalability and optical performance at room temperature. These properties make Ga_2O_3 highly suitable for large scale passivation and protection of monolayer TMDCs in functional heterostructures.

Two-dimensional (2D), atomically thin monolayers of transition metal dichalcogenide crystals (TMDCs) are highly optically active, direct bandgap semiconductors that have emerged as a promising platform for future low-energy electronics, optoelectronics, and photonics [1–4]. Extensive research points to an exceptional potential of TMDC excitons (stable electron-hole pairs) [5] for ultra-efficient energy and information technologies [6, 7], sensing [8], and fundamental studies of collective quantum phenomena [9, 10]. However, integration

This is the author manuscript accepted for publication and has undergone full peer review but has not been through the copyediting, typesetting, pagination and proofreading process, which may lead to differences between this version and the Version of Record. Please cite this article as doi: 10.1002/adma.202005732

This article is protected by copyright. All rights reserved.

Author Manuscript

of monolayer TMDCs into useful electrical and optical devices by direct material deposition, e.g. of high-κ dielectric materials for top-gating [11–13], usually degrades their electronic and optical properties. High optical and electronic performance can be achieved and retained [14, 15] by full encapsulation in mechanically exfoliated hexagonal boron nitride (hBN), commonly used to passivate and protect the monolayers. However, this approach is inherently non-scalable since mechanical exfoliation leads to irregular shaped crystals with inconsistent thickness and size. Significant effort has been directed towards increasing the size of monolayer TMDCs from several μm to the cm-scale [16, 17], and the capability to passivate and protect the monolayers on similar scales is equally important. Without a large scale passivation and protection technology, the realization of multilayer structures with integrated monolayer TMDCs remains challenging and non-scalable.

A practical passivation and protection material should: a) have a uniform, nm-scale thickness on wafer scale, b) have no negative effects on the optical and electrical properties of monolayer TMDCs, and c) protect against further material deposition to enable the integration into multilayer heterostructures. While a large scale passivation of $MoSe_2$ can be achieved by using the larger bandgap TMDC MoS_2 [18], large-scale passivation and protection with a wide-bandgap material, potentially applicable for all TMDCs is not yet available. Here, we introduce an isotropic, ultrathin Ga_2O_3 glass [19] as a novel material for low-cost passivation and protection of atomically-thin semiconductors. Traditionally, research into 2D materials focuses on crystalline materials. Fully amorphous ultrathin materials that feature a glass-like structure are rarely investigated but possess intriguing and useful properties [20]. The wide-bandgap ultrathin Ga_2O_3 glass can be synthesized under ambient conditions, with a highly reproducible nm-scale thickness of less on cm-scale. By capping the notoriously fragile WS_2 with Ga_2O_3, we demonstrate its excellent passivating properties. Our measurements at cryogenic temperatures indicate that the Ga_2O_3 passivates the commercial grade WS_2 monolayer by filling in sulphide vacancies. The passivated WS_2 exhibits enhanced exciton photoluminscence (PL) and suppressed exciton annihilation processes, similarly to the effects of superacid treatment [21] and full hBN encapsulation [22]. Finally, we show that Ga_2O_3 protects WS_2 against further deposition of Al_2O_3, a high-κ dielectric material. Comparison of the exciton PL of commercial grade monolayer WS_2 capped by either Ga_2O_3 or hBN shows that the Ga_2O_3 glass outperforms hBN as a protective material at room temperature.

Amorphous Ga_2O_3 is an electrically insulating, isotropic glass, fully transparent in the visible range [23], and is therefore well suited for protection of optically active materials. The recently discovered liquid metal printing method [19] enables the low-cost synthesis of cm-sized ultrathin sheets of Ga_2O_3 (Figure 1A). Atomic force microscope (AFM) measurements performed on multiple Ga_2O_3 sheets confirm their uniform thickness (t $\approx$

Author Manuscript

This article is protected by copyright. All rights reserved.

2.98 ± 0.10 nm), self-limited by the Cabrera-Mott mechanism [19] [see Supporting Information S1]. X-ray photoelectron spectroscopy (XPS) on the Ga_2O_3 confirms the purity of its stoichiometric composition with 60% oxygen and 40% gallium [see Supporting Information S2]. A scanning electron microscope with a transmission diffraction stage was used to measure the crystal structure of synthesized Ga_2O_3, revealing that it is an entirely amorphous, isotropic glass [see Supporting Information S3] , stable in a wide temperature range [see Supporting Information S4]. Electron energy loss spectroscopy (EELS) measurements unveiled a bandgap of around 5.1 eV [see Supporting Information S5].

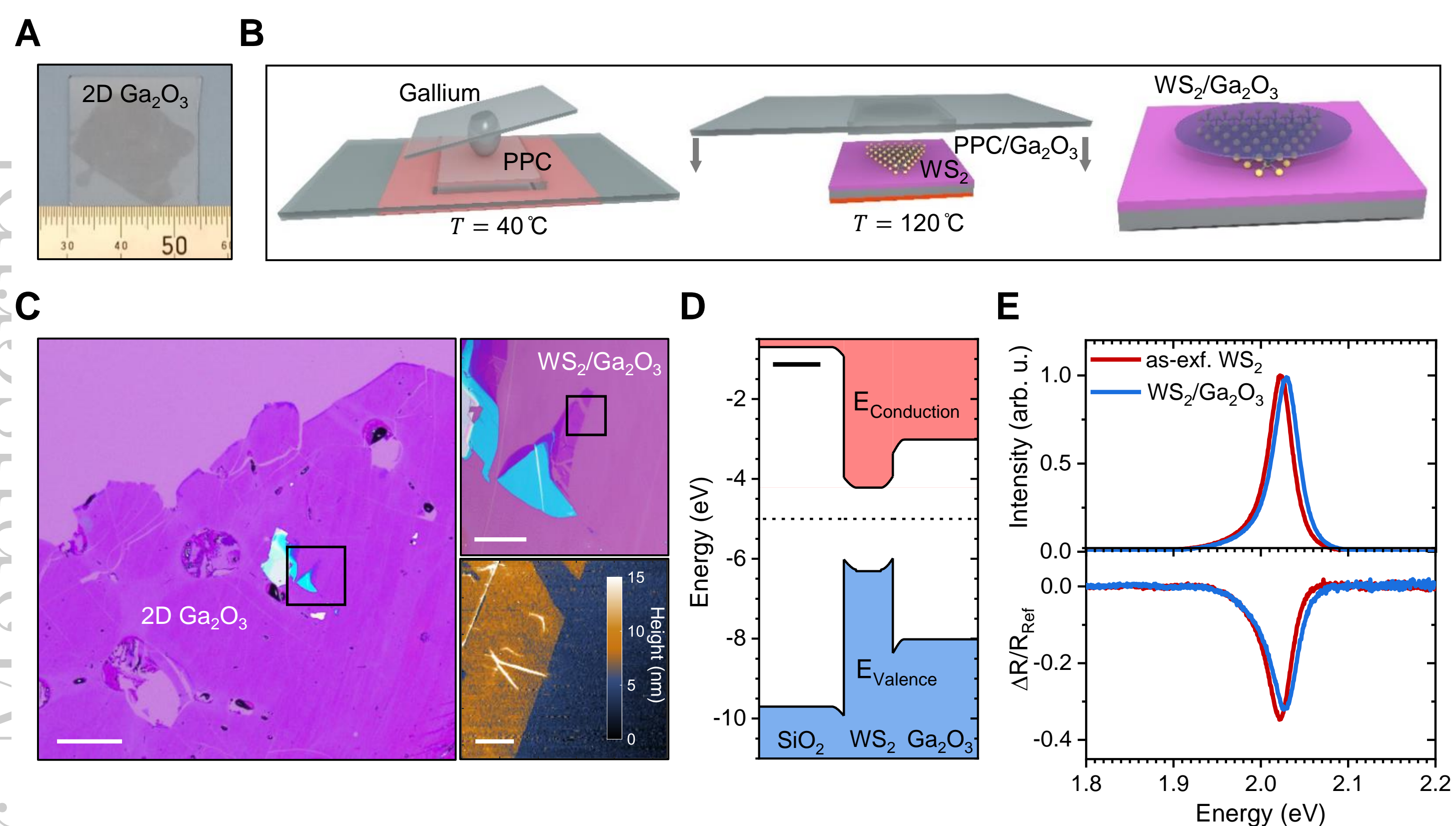

Figure 1: Large scale passivation of monolayer WS_2 with ultrathin Ga_2O_3 glass: (A) Camera image of a cm-sized Ga_2O_3 sheet on glass. The values on the ruler are in the mm scale; (B) Schematics of the PPC-assisted deterministic transfer technique for TMDC/Ga_2O_3 heterostructures (from left to right); (C) Microscope and AFM images of a WS_2/Ga_2O_3 heterostructure (scale bar sizes: 200 μm, 40 μm, and 5 μm). (D) Schematic band diagram of the WS_2/Ga_2O_3 heterostructure (scale bar size: 2 nm), (E) PL and reflectivity spectra of an as-exfoliated monolayer WS_2 and of a WS_2/Ga_2O_3 heterostructure under ambient conditions.

We have developed two high-yield techniques for capping monolayer TMDCs with the Ga_2O_3 glass. The first technique is the direct synthesis of Ga_2O_3 on top of the monolayers, capable of covering large-area TMDCs, e.g. grown by chemical vapor deposition (CVD) [see Supporting Information S6 and S7]. The second technique (Figure 1B) is the deterministic transfer of the Ga_2O_3, synthesized on spin-coated poly-propylene carbonate (PPC), onto target areas, such as μm-sized mechanically exfoliated monolayers [Supporting Information S8]. These methods were used to create the WS_2/Ga_2O_3 heterostructures with both CVD-grown and exfoliated mono-

Author Manuscript

This article is protected by copyright. All rights reserved.

layers. Monolayer WS_2 features the largest band gap in the TMDC family [4], and therefore enables us to test whether Ga_2O_3 glass sufficiently confines the excited charge carriers in the TMDCs. In what follows, we focus on monolayer WS_2 mechanically exfoliated from single-crystalline commercial grade bulk crystals, which have superior optical quality compared to the large-scale CVD-grown monolayers used in this work.

Figure 1C shows a clean mm-scale sheet of Ga_2O_3 deterministically transferred on top of an exfoliated monolayer WS_2 [see Supporting Information S9 for the results on CVD-grown WS_2]. The AFM image of the sample surface shows a homogeneous monolayer coverage. A careful analysis of the step-profile of a WS_2/Ga_2O_3 heterostructure can be found in the Supporting Information S1. The XPS and EELS measurements shown in Supporting Information S1 and S4, together with the known material properties of monolayer WS_2 [24, 25], amorphous SiO_2 [26], and amorphous Ga_2O_3 [23], allow us to construct a band diagram of the WS_2/Ga_2O_3 heterostructure (see Figure 1D), while the exact position of the WS_2 band edge is still under debate [5, 24, 25]. The identified type I band alignment enables the Ga_2O_3 to confine the free carriers in the conduction and valence bands of WS_2, to form excitons.

To test the effect of the Ga_2O_3 capping on the exciton properties of monolayer WS_2, we performed PL and reflectivity studies. The system was excited by a ND:YAG continuous wave (cw) laser source with a wavelength of $\lambda = 532$ nm ($E \approx 2.33$ eV) which is energetically above the band gap of monolayer WS_2, but below the band gap of the ultrathin Ga_2O_3. The reflectivity measurements were performed with a tungsten halogen white light source. The PL and reflectivity spectra of an as-exfoliated monolayer WS_2 and of the WS_2/Ga_2O_3 heterostructure under ambient conditions feature the exciton PL and absorption at $E \approx 2.01$ eV (Figure 1E). The excitons in WS_2/Ga_2O_3 have slightly higher energies compared to the as-exfoliated WS_2, most likely due to dielectric screening effects in Ga_2O_3. Nevertheless, the amplitude and the linewidth of the PL and reflectivity spectra are not affected by Ga_2O_3 capping, indicating that the WS_2 excitons are not quenched. The PL and Raman measurements on the CVD-grown monolayers confirm these results, and show that the optical phonon modes of monolayer WS_2 remain intact [see Supporting Information S9]. By contrast, exciton PL of exfoliated WS_2 monolayers passivated with the commercial grade hBN is significantly quenched [see Supporting Information S10].

The effect of the Ga_2O_3 capping on the WS_2 exciton PL and absorption was further tested at $T = 4.3$ K, when exciton-phonon interactions and thermal effects are suppressed. We excited the as-exfoliated WS_2 and the heterostructure with a large Gaussian laser spot of the diameter $\sim 25\ \mu$m, which effectively eliminated artefacts due to the sample inhomogeneities by averaging the PL over a large sample area. Figure 2A contains the corresponding PL intensity maps, showing that both the as-exfoliated WS_2 and the heterostructure have a homogeneous PL

Author Manuscript

This article is protected by copyright. All rights reserved.

texture. The PL spectra of the monolayers (Figure 2B) are composed of multiple distinct PL peaks, including the exciton ($E_X \approx 2.09$eV), the trion ($E_T \approx 2.06$eV) and additional low energy peaks associated with many-body complexes [4, 27, 28]. The reflectivity spectra (Figure 2C) of the exfoliated monolayers show strong absorption features at the exciton and trion energies, which indicates that both the uncapped and the capped samples are doped [14]. Since the ratios between the absorption dips for both samples are the same, this effect is not related to the Ga_2O_3 capping and can be traced to the large density of sulphide vacancies in the commercial grade monolayer WS_2 resulting in high intrinsic n-type doping [29].

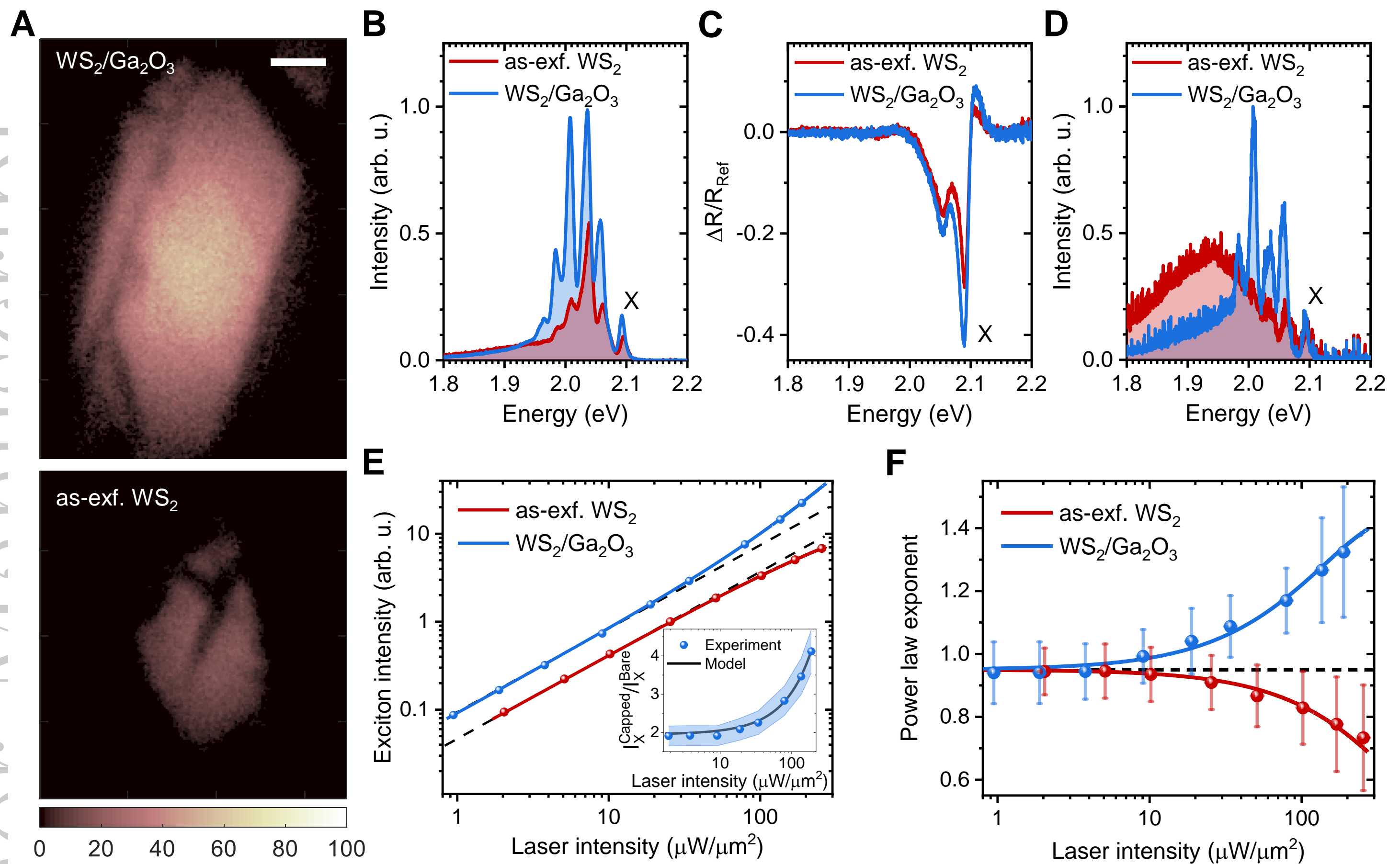

Figure 2: PL studies on a WS_2/Ga_2O_3 heterostructure at $T = 4.3$ K: (A) PL images of a WS_2/Ga_2O_3 heterostructure and of an as-exoliated monolayer WS_2 under large Gaussian laser spot excitation ($\sim$25 μm), the scale bar size is 5 μm; (B) corresponding PL spectra with $I_L \approx 34\ \mu W/\mu m^2$, (C) reflectivity spectra, and (D) PL spectra with $I_L \approx 1.7\ \mu W/\mu m^2$; (E) Laser intensity dependent exciton PL intensities (dots) fitted with the model from the Supporting Information S12 (solid line); (inset) Exciton PL intensity ratios in the bare and the capped monolayers; (F) Extracted power law-exponent k (slope) for the exciton PL intensities. The dashed lines correspond to a power law exponent of $k = 0.95$.

The PL intensity of the heterostructure is strongly enhanced at cryogenic temperatures (see Figure 2A,B and Supporting Information S9, S11). In particular, at low excitation intensities, the broad bound exciton peak, which dominates the PL spectrum of the as-exfoliated sample around 146 meV below the free exciton energy [30], is strongly quenched while the PL of the excitons, trions and low-energy states are enhanced (Figure 2D). This in-

This article is protected by copyright. All rights reserved.

Author Manuscript

dicates that Ga_2O_3 capping suppresses formation of bound excitons at sulphide vacancies [31], enhancing the formation of many-body states and the total exciton quantum yield. Indeed, cathodoluminescene (CL) measurements at $T = 70$ K presented in Supporting Information S12, reveal the presence of deep donor-type oxide vacancies in Ga_2O_3 [32] with a change of the density and distribution of the vacancies in the WS_2/Ga_2O_3 heterostructure. This result suggests that oxides in the Ga_2O_3 passivate sulphide vacancies in the WS_2, possibly through hydrogen-like bonds, changing the density and distribution of the oxygen vacancies in the Ga_2O_3 sheet. This mechanism can explain the suppression of bound exciton formation in the WS_2/Ga_2O_3 without affecting its doping level. The exact nature of the bonding between the WS_2 and the Ga_2O_3 is the subject of future work.

To understand the origins of the PL enhancement, we measured the exciton PL of both the as-exfoliated WS_2 and the WS_2/Ga_2O_3 heterostructure for a range of laser intensities I_L spanning two orders of magnitude (Figure 2E). Corresponding PL spectra are shown in Supporting Information S11. At laser intensities below ~ 10 μW/μm^2, the exciton intensity of the uncapped monolayers follows the power law, $I_X \propto I_L^k$, shown by the dashed lines in Figure 2E. Without losses, and assuming the direct photon-exciton transition, the dependence is linear: $k = 1$ [33]. In our samples, at low laser intensities, $k \approx 0.95$, which indicates that the exciton formation experiences intensity-dependent losses, e.g., free-to-bound exciton transitions or formation of many-body exciton complexes (Figure 2D). However, at laser intensities above ~ 10 μW/μm^2, the exponent of the power law $k \propto \log I_X / \log I_L$ decreases for the as-exfoliated WS_2 (see Figure 2F), in line with previous observations [22]. This behaviour is typically caused by annihilation processes between multiple excitons or between excitons and defects [34], e.g. Auger recombination [35].

In contrast, for the heterostructure the power law exponent remains well above $k \approx 0.95$. This indicates that the exciton annihilation in monolayer WS_2 is suppressed by Ga_2O_3 capping, similarly to the effect of full hBN encapsulation [22, 35]. However, the mere suppression of annihilation would result in a linear power law with a constant $k \approx 1$ [22], while in WS_2/Ga_2O_3 the exciton PL transitions from a linear to a nonlinear behaviour with increasing laser intensities (Figure 3F). This transition can be explained by a two-step exciton generation process via the deep oxide vacancies in the Ga_2O_3 [see Supporting Information S13], in addition to the direct electron-hole excitation. The indirect process involves electron tunnelling between the donor-type oxide vacancies and the WS_2 valence band as an intermediate step in the WS_2 exciton formation. This results in accumulation of exciton densities and growing enhancement of the exciton PL intensity.

By fitting the exciton intensities and the extracted power law exponents of both as-exfoliated WS_2 and the heterostructure (see Figure S2E-F) with the theoretical model [see Supporting Information S13], we deduce that the

This article is protected by copyright. All rights reserved.

Author Manuscript

exciton generation rate in the heterostructure is 1.9 ± 0.3 times higher, and that the exciton saturation density dictated by the annihilation processes is 28 ± 3 times higher compared to the as-exfoliated WS_2. These accumulating effects lead to the observed power-dependent enhancement of the exciton PL intensity in WS_2/Ga_2O_3, with an enhancement factor of 4.1 ± 0.6 within our power range (Figure 2E, inset). Measurements on CVD-grown monolayer WS_2 show the same PL intensity enhancement at cryogenic temperatures [Supporting Information S9].

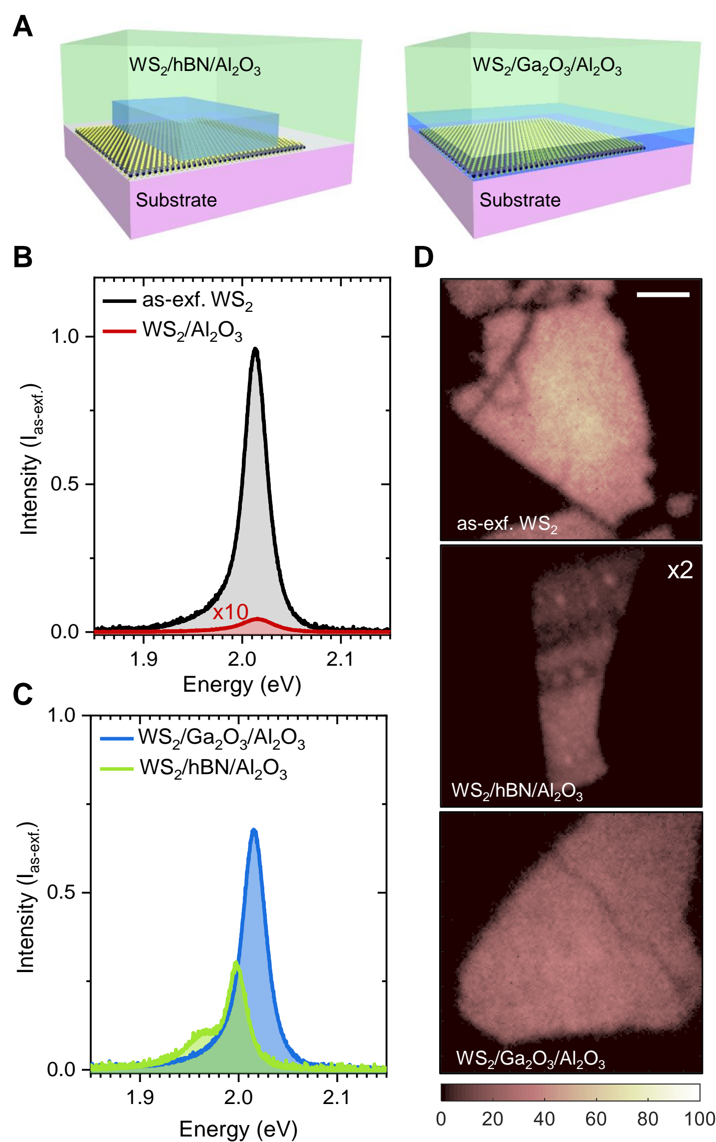

Figure 3: Integration of monolayer WS_2 in a high-κ dielectric environment: (A) Schematics of WS_2/hBN/Al_2O_3 and WS_2/Ga_2O_3/Al_2O_3 heterostructures on SiO_2 substrates; (B) PL spectra of monolayer WS_2 on SiO_2 before (as-exfoliated) and after Al_2O_3 deposition by EBE; (C) PL spectra of WS_2/hBN/Al_2O_3 and WS_2/Ga_2O_3/Al_2O_3 heterostructures; (D) PL intensity maps of as-exfoliated WS_2, and WS_2/hBN/Al_2O_3 and WS_2/Ga_2O_3/Al_2O_3 heterostructures under Gaussian spot excitation ($\sim 25\ \mu m$). PL intensity of WS_2/hBN/Al_2O_3 is multiplied by a factor of 2. The scale bar size is $5\ \mu$m.

To test the protective capacity of the ultrathin Ga_2O_3 for device integration, we deposited Al_2O_3, a high-κ dielectric material, onto monolayer WS_2 capped by either Ga_2O_3 or exfoliated commercial grade hBN (Figure

This article is protected by copyright. All rights reserved.

Author Manuscript

3A). For deposition, we used electron beam evaporation (EBE) with a relatively high electron beam energy to stress-test the protection. As seen in Figure 3B, direct EBE deposition of Al_2O_3 on top of bare WS_2 strongly quenches the exciton PL [11]. The PL spectra (Figure 3C) of the hBN and Ga_2O_3 capped WS_2 after EBE of Al_2O_3 show that both methods protect well against further material deposition, with approximately two orders of magnitude enhancement of exciton PL intensities compared to WS_2/Al_2O_3.

However, the PL spectrum of the hBN-capped WS_2 (Figure 3C) shows a pronounced shoulder at the trion energy ($E_T \approx 1.96$ eV), which indicates that it is strongly doped after Al_2O_3 deposition process, similarly to the effect observed in vacuum [see Supporting Information S9]. In addition, the hBN flake covers the monolayer only partially, resulting in a relatively small protected area (Figure 3D). In contrast, the PL spectrum of the $WS_2/Ga_2O_3/Al_2O_3$ heterostructure shows strong neutral exciton PL with around 70% of the exciton intensity of an as-exfoliated WS_2 monolayer. The PL texture of the $WS_2/Ga_2O_3/Al_2O_3$ is homogeneous (Figure 3D), which highlights the homogeneity of the coverage. The PL measurements on Ga_2O_3-capped CVD-grown monolayer WS_2 support these observations [see Supporting Information S9].

To summarise, the novel ultrathin Ga_2O_3 glass shows great potential as a low-cost and practical wide-bandgap, isotropic material for scalable passivation of monolayer WS_2. Capping the monolayers with Ga_2O_3, either by direct printing or by deterministic transfer, fully preserves their exciton properties in ambient conditions. At cryogenic temperatures, the Ga_2O_3 passivation significantly enhances the optical performance of WS_2 by suppressing bound exciton formation at the sulphide vacancies, promoting nonlinear exciton generation, and suppressing the exciton annihilation processes. These findings provide a pathway towards high-performance surface-passivated TMDC/Ga_2O_3 heterostructures on a cm-scale, e.g., by combining the large-scale mechanical exfoliation [17] with the Ga_2O_3 capping. Finally, our finding that the Ga_2O_3 glass outperforms hBN for protecting commercial grade monolayer WS_2 against high-κ dielectric material deposition (e.g., for top-gating) breaks new ground for the transition from surface TMDC-based devices with small functional areas to large-area devices fully encapsulated in a dielectric environment.

Supporting Information

Supporting Information is available from the Wiley Online Library or from the author.

Acknowledgements

This work was supported by the Australian Research Council (ARC) through the Centre of Excellence grant CE170100039. T.D. acknowledges funds received for the ARC DECRA Project DE190100100. C.S. gratefully acknowledges funding by the European Research Council (Project unLiMIt-2D, Grant No: 679288). B.H and

This article is protected by copyright. All rights reserved.

Author Manuscript

J.M. acknowledge funding in the framework of the German Science Foundation (DFG) project 'BerlinEM Network' (grant number KO2911/13-1) and SFB951 HIOS (project number 182087777), respectively. The authors are grateful to Dr. Aaron Elbourne for providing support with atomic force microscope measurements, to A/Prof. Sumeeet Walia and Dr. Daniel Gomzez for providing access to experimental equipment, and to Mr. Wendi Ma for providing support with sample fabrication. The authors appreciate the use of the Australian National Fabrication Facility (ANFF) at its nodes in the Australian Capital Territory,Victoria and New South Wales.

References

[1] K. F. Mak, J. Shan, *Nature Photonics* **2016**, *10*, 216.

[2] Q. H. Wang, K. Kalantar-Zadeh, A. Kis, J. N. Coleman, M. S. Strano, *Nature Nanotechnology* **2012**, *7*, 699 .

[3] A. K. Geim, I. V. Grigorieva, *Nature* **2013**, *499*, 419.

[4] T. Mueller, E. Malic, *npj 2D Materials and Applications* **2018**, *2*, 29.

[5] A. Chernikov, T. C. Berkelbach, H. M. Hill, A. Rigosi, Y. Li, O. B. Aslan, D. R. Reichman, M. S. Hybertsen, T. F. Heinz, *Physical Review Letters* **2014**, *113*, 076802.

[6] K. F. Mak, K. L. McGill, J. Park, P. L. McEuen, *Science* **2014**, *344*, 1489.

[7] B. Radisavljevic, A. Radenovic, J. Brivio, V. Giacometti, A. Kis, *Nature Nanotechnology* **2011**, *6*, 147.

[8] S. Manzeli, D. Dumcenco, G. Migliato Marega, A. Kis, *Nature Communications* **2019**, *10*, 4831.

[9] Z. Wang, D. A. Rhodes, K. Watanabe, T. Taniguchi, J. C. Hone, J. Shan, K. F. Mak, *Nature* **2019**, *574*, 76.

[10] M. M. Fogler, L. V. Butov, K. S. Novoselov, *Nature Communications* **2014**, *5*, 4555.

[11] S. Y. Kim, H. I. Yang, W. Choi, *Applied Physics Letters* **2018**, *113*, 133104.

[12] K. M. Price, S. Najmaei, C. E. Ekuma, R. A. Burke, M. Dubey, A. D. Franklin, *ACS Applied Nano Materials* **2019**, *2*, 4085.

[13] J.-G. Song, S. J. Kim, W. J. Woo, Y. Kim, I.-K. Oh, G. H. Ryu, Z. Lee, J. H. Lim, J. Park, H. Kim, *ACS Applied Materials and Interfaces* **2016**, *8*, 28130.

[14] M. Sidler, P. Back, O. Cotlet, A. Srivastava, T. Fink, M. Kroner, E. Demler, A. Imamoglu, *Nature Physics* **2017**, *13*, 255.

This article is protected by copyright. All rights reserved.

Author Manuscript

[15] J. Gu, B. Chakraborty, M. Khatoniar, V. M. Menon, *Nature nanotechnology*, **2019**, *14*, 1024.

[16] J. Lee, S. Pak, P. Giraud, Y.-W. Lee, Y. Cho, J. Hong, A-R. Jang, H.-S. Chung, W.-K. Hong, H. Y. Jeong, H. S. Shin, L. G. Occhipinti, S. M. Morris, S. N. Cha, J. I. Sohn, J. M. Kim, *Advanced Materials* **2017**, *29*, 1702206.

[17] F. Liu, W. Wu, Y. Bai, S. H. Chae, Q. Li, J. Wang, J. Hone, X.-Y. Zhu, *Science* **2020**, *367*, 903.

[18] A. Surrente, D. Dumcenco, Z. Yang, A. Kuc, Y. Jing, T. Heine, Y.-C. Kung, D. K. Maude, A. Kis, P. Plochocka, *Nano Letters* **2017**, *17(7)*, 4130.

[19] A. Zavabeti, J. Z. Ou, B. J. Carey, N. Syed, R. Orell-Trigg, E. L. H. Mayes, C. Xu, O. Kavehei, A. P. O'Mullane, R. B. Kaner, K. Kalantar-zadeh, T. Daeneke, *Science* **2017**, *358*, 332.

[20] C.-T. Toh, H. Zhang, J. Lin, A. S. Mayorov, Y.-P. Wang, C. M. Orofeo, D. B. Ferry, H. Andersen, N. Kakenov, Z. Guo, I. H. Abidi, H. Sims, K. Suenaga, S. T. Pantelides, B. Özyilmaz, *Nature* **2020**, *577*, 199.

[21] M. Amani, D.-H. Lien, D. Kiriya, J. Xiao, A. Azcatl, J. Noh, S. R. Madhvapathy, R. Addou, S. KC, M. Dubey, K. Cho, R. M. Wallace, S.-C. Lee, J.-H. He, J. W. Ager III, X. Zhang, E. Yablonovitch, A. Javey, *Science* **2015**, *350*, 1065.

[22] Y. Hoshi, T. Kuroda, M. Okada, R. Moriya, S. Masubuchi, K. Watanabe, T. Taniguchi, R. Kitaura, T. Machida, *Physical Review B* **2017**, *95*, 241403(R).

[23] J. Kim, T. Sekiya, N. Miyokawa, N. Watanabe, K. Kimoto, K. Ide, Y. Toda, S. Ueda, N. Ohashi, H. Hiramatsu, H. Hosono, T. Kamiya , *NPG Asia Materials* **2017**, *9*, e359.

[24] H. L. Zhuang, R. G. Hennig, Computational Search for Single-Layer Transition-Metal Dichalcogenide Photocatalysts, *J. Phys. Chem. C* **2013**, *117*, 40, 20440.

[25] H. Terrones, F. López-Urías, M. Terrones, Novel hetero-layered materials with tunable direct band gaps by sandwiching different metal disulfides and diselenides, *Scientific Reports* **2013**, *3*, 1549.

[26] V. Astašauskas, A. Bellissimo, P. Kuksa, C. Tomastik, H. Kalbe, W. S. M. Werner, *Journal of Electron Spectroscopy and Related Phenomena* **2020**, *241*, 146829.

[27] P. Nagler, M. V. Ballottin, A. A. Mitioglu, M. V. Durnev, T. Taniguchi, K. Watanabe, A. Chernikov, C. Schüller, M. M. Glazov, P. C. M. Christianen, T. Korn, *Physical Review Letters* **2018**, *121*, 057402.

Author Manuscript

This article is protected by copyright. All rights reserved.

[28] S.-Y. Chen, T. Goldstein, T. Taniguchi, K. Watanabe, J. Yan, *Nature Communications* **2018**, *9*, 3717.

[29] S.-S. Chee, C. Oh, M. Son, G.-C. Son, H. Jang, T. J. Yoo, S. Lee, W. Lee, J. Y. Hwang, H. Choi, B. H. Lee, M.-H. Ham, *Nanoscale* **2017**, *9*, 9333.

[30] C. Cong, J. Shang, Y. Wang, T. Yu, *Advanced Optical Materials* **2018**, *6*, 1700767.

[31] V. Carozo, Y. Wang, K. Fujisawa, B. R. Carvalho, A. McCreary, S. Feng, Z. Lin, C. Zhou, N. Perea-López, A. L. Elías, B. Kabius, V. H. Crespi, M. Terrones, *Science Advances* **2017**, *3*, e1602813.

[32] J. B. Varley, J. R. Weber, A. Janotti, C. G. V. d. Walle, Oxygen vacancies and donor impurities in β-Ga_2O_3, *Applied Physics Letters* **2010**, *97*, 142106.

[33] C. Spindler, T. Galvani, L. Wirtz, G. Rey, S. Siebentritt, *Journal of Applied Physics* **2019**, *126*, 175703.

[34] G. Moody, J. Schaibley, X. Xu, *Journal of the Optical Society of America B* **2016**, *33*, C39.

[35] J. Zipfel, M. Kulig, R. Perea-Causín, S. Brem, J. D. Ziegler, R. Rosati, T. Taniguchi, K. Watanabe, M. M. Glazov, E. Malic, A. Chernikov, *Physical Review B* **2020**, *101*, 115430.

Author Manuscript

This article is protected by copyright. All rights reserved.